arXiv:1608.01625v2 [cond-mat.stat-mech] 5 Mar 2017

Coarsening dynamics of zero-range processes

Claude Godrèche and Jean-Michel Drouffe

Institut de Physique Théorique, Université Paris-Saclay, CEA and CNRS, 91191 Gif-sur-Yvette, France

Abstract. We consider a class of zero-range processes exhibiting a condensation transition in the stationary state, with a critical single-site distribution decaying faster than a power law. We present the analytical study of the coarsening dynamics of the system on the complete graph, both at criticality and in the condensed phase. In contrast with the class of zero-range processes with critical single-site distribution decaying as a power law, in the present case the role of finite-time corrections are essential for the understanding of the approach to scaling.

1. Introduction

While the static properties of zero-range processes (ZRP) are by now well understood [1, 2, 3, 4], dynamical properties are far less investigated. This is all the more true when the model exhibits a condensation transition in the stationary state. In such instances, of particular interest is the long-time evolution of the system starting from a homogeneous disordered initial condition. In the scaling regime, a coarsening phenomenon takes place, i.e., a group of sites, whose number decreases, progressively become more populated, a process followed in the late-time regime by the appearance of a condensate. A few studies have been devoted in the past to the coarsening dynamics of the class of ZRP with a single-site critical distribution decaying as a power law [5, 6, 7, 8]. These studies yield analytical results when the dynamics takes place on the complete graph and in the thermodynamical limit [5, 6, 7]. In contrast, the knowledge of the dynamics of the one-dimensional system only relies on numerical work and heuristic arguments [7, 8]. When the density is just equal to the critical density one rather speaks of critical coarsening, which is the process by which dynamics progressively establishes the critical state [6, 7].

The present work is a sequel of [7] and of the related works [5, 6]. Following the same line of thought, we investigate the dynamics of a different class of ZRP, for which the critical single-site distribution at stationarity decays faster than a power law. Again, analytical results can be obtained on the complete graph and in the thermodynamical limit. The novelty of this case comes from the fact that, though the asymptotic scaling functions associated to the single-site distributions are simpler than in the power-law case, the approach to scaling is more complicated. The analysis of this phenomenon is the main goal of the present work.

We proceed as in [7], analysing the coarsening dynamics of the system, first at criticality, then in the condensed phase. For both cases, we give an analytical treatment of the equations describing the temporal evolution of the single-site

occupation probability in the continuum scaling limit. For the critical phase, finite-time corrections to scaling can be explicitly determined. The parallel study of the condensed phase turns out to be much harder. We use a semi-classical analysis of the differential equation describing the coarsening regime, in order to study the corrections to scaling.

The same model was recently investigated in [9], with focus on coarsening in the condensed phase. We shall review this work in the discussion at the end of the present paper. A list of mathematical references on related issues can be found in [9].

2. Definition of the model

Consider a finite connected graph, made of L sites, $i = 1, \ldots, L$. At time t, on each site we have $N_i(t)$ indistinguishable particles such that

$$\sum_{i=1}^{L} N_i(t) = N. \tag{2.1}$$

The dynamics of the system is given by the rate $W(d, a, k, \ell)$ at which a particle leaves the departure site with label d, containing $N_d = k$ particles, and is transferred to the arrival site with label a containing $N_a = \ell$ particles. By definition of a ZRP, this hopping rate does not depend on the occupation of the arrival site and takes the simple form

$$W(d, a, k) = w_{d,a} u_k, \tag{2.2}$$

where $w_{d,a}$ accounts for diffusion from site d to site a and u_k only depends on the occupation of the departure site. In the present work we consider the complete graph where, by definition, all sites are connected. We take $w_{d,a} = 1/L$, i.e., all sites are equivalent and the system is spatially homogeneous. We choose the rate

$$u_k = 1 + \frac{b}{k^\sigma}, \tag{2.3}$$

where $0 < \sigma < 1$ is an arbitrary exponent. This form of the rate appeared in the past in several publications, such as [3, 10, 11]. It satisfies the criterion for condensation to occur [12] for any value of b. In contrast, for the ZRP with rate $u_k = 1 + b/k$, hereafter referred to as the $\sigma = 1$ case, condensation only occurs for $b > 2$.

We denote a configuration of the system at time t by $\{n_i\} \equiv (n_1, n_2, \ldots, n_L)$, where the $n_i = 0, 1, 2, \ldots$ are the values taken by the occupation numbers $N_i(t)$. Thus, the complete knowledge of its dynamics involves the determination of the probability $\mathcal{P}(\{n_i\})$ of finding the system in the given configuration $\{n_i\}$ at time t. Hereafter we will focus our attention on a marginal of this distribution, namely on the probability of finding k particles on the generic site $i = 1$, that, for short, we shall name the (single-site) occupation probability,

$$f_k(t) = \mathcal{P}(N_1(t) = k) = \langle \delta(N_1(t), k) \rangle \tag{2.4}$$

$$= \sum_{n_1, \ldots, n_L} \delta(n_1, k) \mathcal{P}(\{n_i\}). \tag{2.5}$$

Conservation of probability and of density implies

$$\sum_{k \geq 0} f_k(t) = 1, \tag{2.6}$$

$$\sum_{k \geq 1} k\, f_k(t) = \langle N_1(t) \rangle = \frac{N}{L}. \tag{2.7}$$

In the thermodynamic limit ($N \to \infty, L \to \infty$, with fixed density $\rho = N/L$) the last equation yields

$$\sum_{k\geq 1} k\, f_k(t) = \rho. \tag{2.8}$$

Let us remind some well-known results on the stationary state of the ZRP [3, 4, 8]. The weight of a configuration is given by

$$\mathcal{P}(\{n_i\}) = \frac{1}{Z_{L,N}} \prod_{i=1}^{L} p_{n_i}, \tag{2.9}$$

where

$$p_0 = 1, \qquad p_k = \frac{1}{u_1 \dots u_k}, \tag{2.10}$$

and where the normalisation factor $Z_{L,N}$ reads

$$Z_{L,N} = \sum_{\{n_i\}} \prod_{i=1}^{L} p_{n_i}\, \delta\left(\sum_{i=1}^{L} n_i, N\right). \tag{2.11}$$

For the rate (2.3) equation (2.10) leads to the estimate, for $k \gg 1$,

$$p_k \sim \exp\left(-b \sum_{\ell=1}^{k} \frac{1}{\ell^\sigma}\right) \sim \exp\left(-\frac{b}{1-\sigma}\, k^{1-\sigma}\right). \tag{2.12}$$

In the thermodynamic limit, this ZRP is condensing whenever the density is larger than the critical density (see figure 1),

$$\rho_c = \frac{\sum_{k\geq 1} k\, p_k}{\sum_{k\geq 0} p_k}. \tag{2.13}$$

The excess density $\rho - \rho_c$ corresponds to the condensate. At the critical density, the occupation probabilities

$$f_{k,\mathrm{eq}} = \frac{p_k}{\sum_{k\geq 0} p_k} \tag{2.14}$$

decay as the stretched exponential law (2.12). Simple derivations of the above results can be obtained in the framework of the next section.

3. Master equation

From now on we consider the thermodynamic limit of the system on the complete graph. In this mean-field geometry the temporal evolution of the occupation probabilities $f_k(t)$ is explicitly given by the master equation

$$\frac{\mathrm{d}f_k(t)}{\mathrm{d}t} = u_{k+1}\, f_{k+1} + \bar{u}_t\, f_{k-1} - (u_k + \bar{u}_t) f_k \qquad (k \geq 1), \tag{3.1}$$

$$\frac{\mathrm{d}f_0(t)}{\mathrm{d}t} = u_1\, f_1 - \bar{u}_t f_0, \tag{3.2}$$

where

$$\bar{u}_t = \sum_{k=1}^{\infty} u_k f_k(t) \tag{3.3}$$

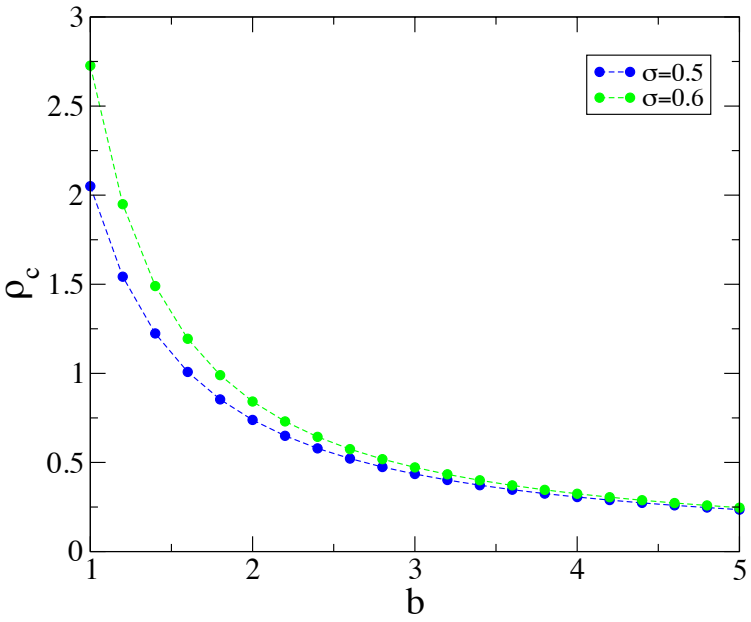

Figure 1. Critical density ρ_c for the ZRP (2.3) for two values of σ.

is the rate at which a particle arrives on site number 1 from any other site. It is the equation for a biased random walk for N_1 (or birth and death process) on the positive integers $k = 0, 1, \ldots$. The rates of a jump to the right ($N_1 = k \to N_1 = k + 1$) or to the left ($N_1 = k \to N_1 = k - 1$) are respectively given by $\bar{u}_t$ and by u_k. The equation for $f_0(t)$ is special because one cannot select an empty site as a departure site, nor can N_1 be negative. This random walk has the peculiar property of being constrained to have its average position fixed at the value ρ (see (2.8)).

The form of the master equation (3.1) is a direct consequence of the mean-field geometry. It has the structure of the master equation for two sites [4], where the role of the second site is here played by the ensemble of all sites, through the self-consistency condition (3.3). This condition implies that (3.1) is non linear because the rate $\bar{u}_t$ is itself a function of the $f_k(t)$. Hence there is no explicit solution of the master equation in closed form. Yet one can extract from (3.1) an analytical description of the dynamics at long times, both at criticality and in the condensed phase, as will be seen in the next sections. This master equation, (or closely related equations), appeared in previous works [5, 6, 7] (see also [13]).

In the stationary state we have

$$\lim_{t\to\infty} \bar{u}_t = \sum_{k\geq 1} u_k f_{k,\mathrm{eq}} = z, \tag{3.4}$$

introducing the short notation z for the limit. Setting the left side of (3.1) and (3.2)

to zero ($\dot{f}_k = 0$) we obtain

$$\frac{f_{k+1,\mathrm{eq}}}{f_{k,\mathrm{eq}}} = \frac{z}{u_{k+1}}, \tag{3.5}$$

which expresses the detailed balance condition at equilibrium. So

$$f_{k,\mathrm{eq}} = z^k p_k f_{0,\mathrm{eq}}, \tag{3.6}$$

where the p_k are given by (2.10) and $f_{0,\mathrm{eq}}$ is fixed by the normalisation (2.6). Hence finally,

$$f_{k,\mathrm{eq}} = \frac{z^k p_k}{\sum_{k\geq 0} z^k p_k}. \tag{3.7}$$

Let $P(z)$ denote the generating series of the p_k appearing in the denominator. The second sum rule (2.8) imposes that

$$\rho = \frac{\sum_{k\geq 1} z^k k p_k}{\sum_{k\geq 0} z^k p_k} = \frac{zP'(z)}{P(z)}. \tag{3.8}$$

This equation determines z as a function of the density. With the choice (2.3), the p_k decay as (2.12), implying that the maximal value of the right side of (3.8), reached at $z = 1$, is finite. This finite value is the critical density (2.13),

$$\sum_{k\geq 1} k f_{k,\mathrm{eq}} = \rho_c. \tag{3.9}$$

We thus recover well-known results of the statics of the ZRP, either in the canonical or in the grand canonical formalisms, which are equivalent in the thermodynamical limit [3, 8].

Here we shall always keep time finite, even if very large, meaning that we are investigating the non-stationary regime, where the system stays homogeneous (in average, not configuration by configuration), allowing to follow the establishement of critical order, or to follow precursor effects of condensation. Let us emphasize that (3.1) can only account for the situation where all sites play the same role. In other words, in the presence of a condensation transition, i.e., when $\rho > \rho_c$, this equation only accounts for the regime of the formation of the condensate. Otherwise stated, in the thermodynamical limit, the non-stationary regime never ends, since the scale of time beyond which the stationary regime begins diverges with the system size L [7, 11].

4. Critical coarsening

We consider the ZRP with hopping rate u_k (2.3), evolving on the complete graph from an homogeneous disordered initial condition specified by $f_k(0)$. For instance, initially particles are distributed at random amongst sites, with an initial density $\rho = \rho_c$, i.e., we consider a system with a Poissonian initial distribution of occupation probabilities,

$$f_k(0) = \mathrm{e}^{-\rho}\frac{\rho^k}{k!}. \tag{4.1}$$

We investigate the critical coarsening process, i.e., the process by which dynamics progressively establishes the critical state. The line of reasoning is similar to that followed in [6, 7].

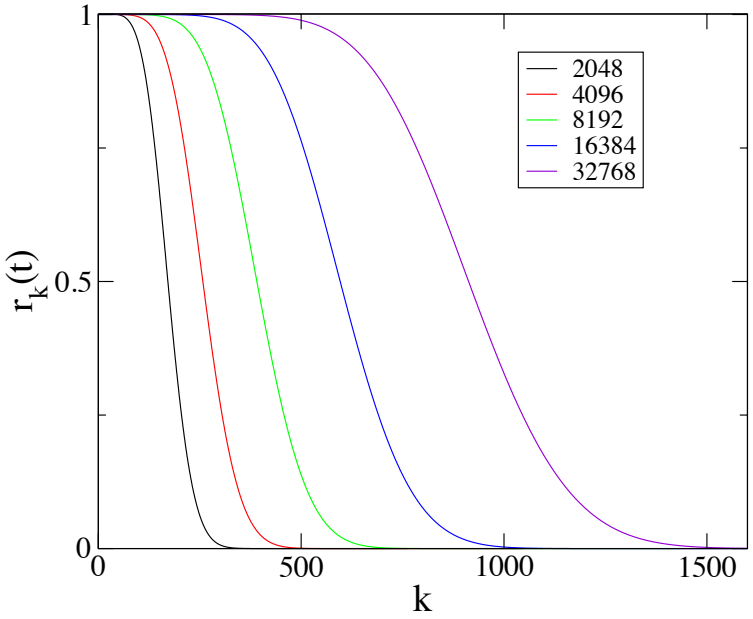

Figure 2. Critical ratio $r_k(t) = f_k(t)/f_{k,\mathrm{eq}}$ for $t = 2048, 4096, \ldots, 32768$, obtained by numerical integration of the discrete master equation (3.1). Here $\sigma = 0.6$, $b = 1$.

Since the average rate $\bar{u}_t$ at which a particle leaves a generic site reaches its equilibrium value $z = 1$ at large times, we set

$$\bar{u}_t = 1 + \eta_t, \tag{4.2}$$

where the small scale η_t will be determined hereafter. Morevover, we are led to investigate the dynamics according to two time-occupancy regimes, as in [6, 7]. These regimes are defined as follows.

(I) *k fixed, t large* In this situation there is convergence to the equilibrium fluid phase. Hence we set

$$f_k(t) = f_{k,\mathrm{eq}}(1 + w_k(t)), \tag{4.3}$$

with $f_{k,\mathrm{eq}}$ given by (2.14) and where the $w_k(t)$ are proportional to η_t as demonstrated below.

(II) *k and t are simultaneously large* This is a regime where scaling is expected, so we look for a solution to (3.1) of the form

$$f_k(t) = f_{k,\mathrm{eq}}\, g(x,t), \qquad x = k\,\varepsilon_t, \tag{4.4}$$

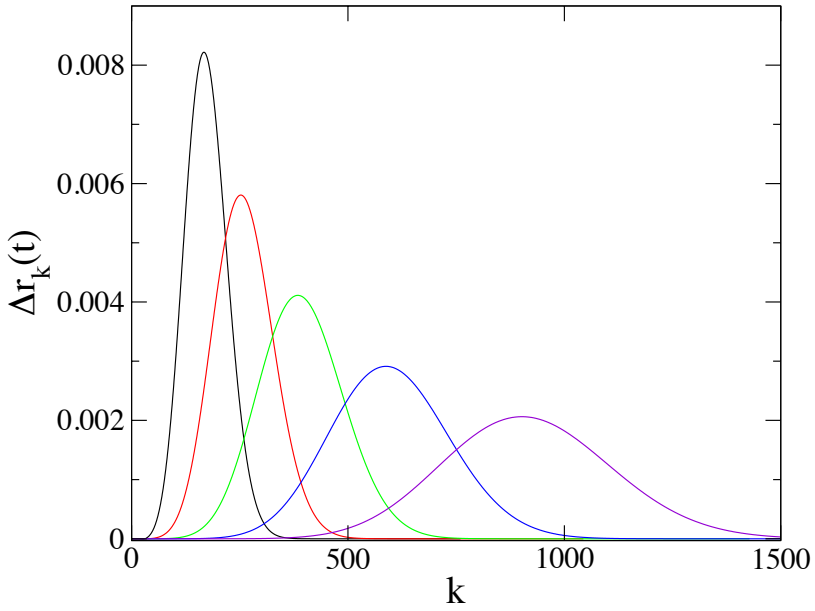

Figure 3. Differences $r_k(t) - r_{k+1}(t)$ for $t = 2048, 4096, \ldots, 32768$, obtained from the data of figure 2.

where ε_t is a small scale, to be determined, x is the scaling variable, and $g(x,t)$ is expected to converge to the scaling function $g(x)$ in the limit of large times.

The present situation is closely related to critical coarsening for a ferromagnetic spin system quenched from infinite temperature down to T_c [14, 15, 16]. In such circumstances, spatial correlations develop in the system, just as in the critical state, but only over a length scale which grows like t^{1/z_c}, where z_c is the dynamic critical exponent. On scales smaller than t^{1/z_c} the system appears critical, while on larger scales the system is still disordered. For instance, for Ising spins, $\sigma = \pm 1$, the equal-time correlation function $C(r,t) = \langle \sigma_0(t)\sigma_r(t)\rangle$ scales as

$$C(r,t) \approx r^{-2\beta/\nu} g\left(\frac{r}{t^{1/z_c}}\right), \tag{4.5}$$

where β and ν are the usual static exponents. The scaling function $g(x)$ goes to a constant as $x \to 0$, while it falls off very rapidly when $x \to \infty$.

Here, anticipating on what follows, starting from a homogeneous disordered initial condition, for a large but finite time t, and for k much smaller than an ordering size of order $t^{1/z}$ (where the exponent z is determined hereafter), the system looks critical, i.e., the distribution $f_k(t)$ has essentially converged toward the equilibrium distribution $f_{k,\mathrm{eq}}$. To the contrary, for $k \gg t^{1/z}$, the system still looks disordered, i.e., the $f_k(t)$ fall off very fast. This is illustrated by figure 2, obtained by numerical integration

of (3.1), which depicts the ratio

$$r_k(t) = \frac{f_k(t)}{f_{k,\mathrm{eq}}}. \tag{4.6}$$

As time increases, this ratio exhibits a plateau of increasing length, reflecting the fact that the system equilibrates. Then this ratio falls down very fast.

The agenda is now to determine the quantities η_t, $w_k(t)$, ε_t, $g(x,t)$, using the sum rules (2.6) and (2.8), the master equations (3.1) and (3.2), and finally the assumptions (4.3) and (4.4). We proceed as follows.

4.1. Time-occupancy regime (I)

The expression (4.3) carried into (3.1), (3.2) imposes the left side $\dot{f}_k$ to vanish because it is proportional to $\dot{w}_k$, which is negligible compared to the right side of (3.1), (3.2). We thus obtain the quasi-stationary condition

$$\frac{f_{k+1,\mathrm{eq}}}{f_{k,\mathrm{eq}}}\frac{1+w_{k+1}}{1+w_k} = \frac{1+\eta_t}{u_{k+1}}, \tag{4.7}$$

which formally resembles the detailed balance condition (3.5) and yields $w_{k+1} - w_k = \eta_t$. Setting $w_k = v_k\eta_t$ we obtain

$$v_k = v_0 + k, \tag{4.8}$$

where v_0 is determined below (see (4.37)).

4.2. Time-occupancy regime (II)

We now turn to the differential equation obeyed by $g(x,t)$. The ratio $r_k(t) = f_k(t)/f_{k,\mathrm{eq}}$ satisfies the equations

$$\frac{\mathrm{d}r_k(t)}{\mathrm{d}t} = r_{k+1} + \bar{u}_t\, u_k\, r_{k-1} - (\bar{u}_t + u_k)r_k \qquad (k \le 1), \tag{4.9}$$

$$\frac{\mathrm{d}r_0(t)}{\mathrm{d}t} = r_1 - \bar{u}_t r_0. \tag{4.10}$$

Using (4.4), the left side of (4.9) becomes

$$\frac{\mathrm{d}g(x,t)}{\mathrm{d}t} = g'\frac{\mathrm{d}x}{\mathrm{d}t} + \dot{g} = g'k\dot{\varepsilon}_t + \dot{g}, \tag{4.11}$$

and the right side yields

$$\begin{aligned} &r_{k+1} + r_{k-1} - 2r_k - \left(\eta_t + \frac{b}{k^\sigma}\right)(r_k - r_{k-1}) + \eta_t\frac{b}{k^\sigma}r_{k-1} \\ &\approx \varepsilon_t^2\, g'' - \left(\frac{\eta_t}{\varepsilon_t^\sigma} + \frac{b}{x^\sigma}\right)\varepsilon_t^{1+\sigma} g' + \eta_t\varepsilon_t^\sigma\frac{b}{x^\sigma}(g + \cdots). \end{aligned} \tag{4.12}$$

As will be shown below, the small scale η_t is decaying exponentially fast. Dropping the corresponding terms in the equation, we obtain the partial differential equation

$$\dot{g} = \varepsilon_t^2\, g'' - \left(\frac{b}{x^\sigma}\varepsilon_t^{1+\sigma} + x\frac{\dot{\varepsilon}_t}{\varepsilon_t}\right) g'. \tag{4.13}$$

In order to equate the powers of ε_t in the second term of the right side, we set, (see also (5.17)),

$$\varepsilon_t = t^{-1/(1+\sigma)}. \tag{4.14}$$

We finally obtain the equation obeyed by $g(x,t)$,

$$t\dot{g} = t^{-a}\, g'' + \left(\frac{x}{1+\sigma} - \frac{b}{x^\sigma}\right) g', \tag{4.15}$$

with

$$a = \frac{1-\sigma}{1+\sigma}. \tag{4.16}$$

By setting $\sigma = 1$, we recover the equation found in [6, 7] for the case $u_k = 1 + b/k$ (see (A.3)), up to the left side of (4.15), which was omitted in these references, since the finite-time corrections need not be considered. We now analyse equation (4.15).

(a) Scaling function At large times, the asymptotic scaling function

$$g(x) = \lim_{t\to\infty} g(x,t) \tag{4.17}$$

satisfies the equation

$$\left(\frac{x}{1+\sigma} - \frac{b}{x^\sigma}\right) g'(x) = 0. \tag{4.18}$$

Hence $g(x) = 1$ as long as the factor in parenthesis does not vanish. This occurs for

$$x = x_0 = [b(1+\sigma)]^{1/(1+\sigma)}. \tag{4.19}$$

For $x > x_0$, $g(x) = 0$. The limiting scaling function is thus a discontinuous curve, depicted in figure 4. In contrast, as can be seen on figure 4, at finite time the solution of (4.15) is a smooth curve, that we now investigate.

Remark Setting $\sigma = 1$ in (4.19) yields $x_0 = \sqrt{2b}$. This prediction matches the result obtained for the ZRP with rate $u_k = 1 + b/k$ in the limit $b \to \infty$ [6]. Indeed, in this limit, the scaling function $g(x)$ becomes a discontinuous front at position $\sqrt{2b}$, as can be seen on its explicit expression (A.4).
This matching between the two ZRP (corresponding respectively to the rates $u_k = 1 + b/k^\sigma$ and $u_k = 1 + b/k$) can be informally summarized as

$$\lim_{\sigma\to 1} \mathrm{ZRP}_{\sigma<1} \sim \lim_{b\to\infty} \mathrm{ZRP}_{\sigma=1}. \tag{4.20}$$

This property can be intuitively understood by noting that, in the limit $b \to \infty$, the decay of the $p_k \sim k^{-b}$ of the second ZRP (with $\sigma = 1$) is formally faster than a power law, thus falling into the class of the first ZRP (with $\sigma < 1$). The same matching will be encountered when investigating coarsening in the condensed phase (see the comment below (6.28)).

(b) Finite-time corrections Consider, for a while, equation (4.15) without its left side. This yields immediately

$$-g'(x,t) \propto \mathrm{e}^{-t^a \psi(x)}, \quad \psi(x) = \int \mathrm{d}x \left(\frac{x}{1+\sigma} - \frac{b}{x^\sigma}\right). \tag{4.21}$$

It turns out that this expression does not account faithfully for the solution of the master equation (3.1) as is demonstrated by what follows. In other words, in order to account for the correct finite-time corrections to the scaling function $g(x)$, both terms

$t\dot{g}$ and $t^{-a}g''$ should be kept. However (4.21) puts us on the path of the correct ansatz for the solution of (4.15). Let us set

$$-g'(x,t) \propto \mathrm{e}^{-t^a \varphi(x)}, \tag{4.22}$$

where $\varphi(x_0) = 0$, since $g'(x,t)$ peaks at x_0 when $t \to \infty$. If we substitute (4.22) in (4.15) we find a differential equation for the function $\varphi(x)$,

$$\varphi' + a\frac{\varphi}{\varphi'} = \frac{x}{1+\sigma} - \frac{b}{x^\sigma}. \tag{4.23}$$

This differential equation does not seem to be of a known type [17]. Nevertheless the behaviours of $\varphi(x)$ at $x \to 0$ or $x \to \infty$ can be predicted,

$$\varphi(x) \underset{x\to 0}{\approx} \varphi(0) - \frac{b x^{1-\sigma}}{1-\sigma}, \quad \varphi(x) \underset{x\to\infty}{\approx} \frac{x^2}{4}. \tag{4.24}$$

A plot of $\varphi(x)$, obtained by a numerical integration of (4.23), is given in figure 6, which is in complete agreement with the data coming from the numerical integration of (3.1), as will be commented later.

We can perform a local analysis of the behaviour of $g'(x,t)$ around x_0, using the expansion

$$\varphi(x) \approx \frac{1}{2}\varphi''(x_0)(x-x_0)^2. \tag{4.25}$$

Cast into (4.23), we obtain the relation

$$\varphi''(x_0) = 1 - \frac{a}{2}. \tag{4.26}$$

Since, at large times, $g(0,t) \to 1$, we impose the normalisation

$$\int_0^\infty \mathrm{d}x\, g'(x,t) = -1. \tag{4.27}$$

So (4.22) yields

$$g'(x,t) \approx -\sqrt{\frac{(1-a/2)t^a}{2\pi}}\mathrm{e}^{-(1-a/2)t^a(x-x_0)^2/2}. \tag{4.28}$$

Hence

$$\begin{aligned} g(x,t) &\approx -\int_x^\infty \mathrm{d}u\, g'(u,t) = \frac{1}{2}\operatorname{erfc}\frac{\sqrt{(1-a/2)}\, t^{a/2}(x-x_0)}{\sqrt{2}} \\ &= \frac{1}{2}\operatorname{erfc}\xi, \end{aligned} \tag{4.29}$$

defining the new scaling variable ξ as

$$\xi = \frac{t^{a/2}(x-x_0)}{\sqrt{2/(1-a/2)}} = \frac{k-k_{\mathrm{typ}}}{\sqrt{2t/(1-a/2)}}, \tag{4.30}$$

and where the typical location of the front depicted in figure 2 is

$$k_{\mathrm{typ}} = x_0 t^{1/(1+\sigma)}. \tag{4.31}$$

So, the front moves more rapidly (as $t^{1/(1+\sigma)}$) than it widens (as $t^{1/2}$). The difference between the two exponents is

$$\frac{1}{1+\sigma} - \frac{1}{2} = \frac{a}{2}, \tag{4.32}$$

which is precisely the exponent appearing in the scaling variable ξ. To summarize, the bulk of the function $g(x,t)$ is given by $(1/2)\operatorname{erfc}\xi$, hence $-g'(x,t)$ is a Gaussian, and the large deviations of the latter are given by (4.22), where $\varphi(x)$ is the large-deviation function.

Remark For k and t large, using the results above, we get $f_k(t) \sim \mathrm{e}^{-k^2/(4t)}$, as for the case $u_k = 1 + b/k$, see Appendix.

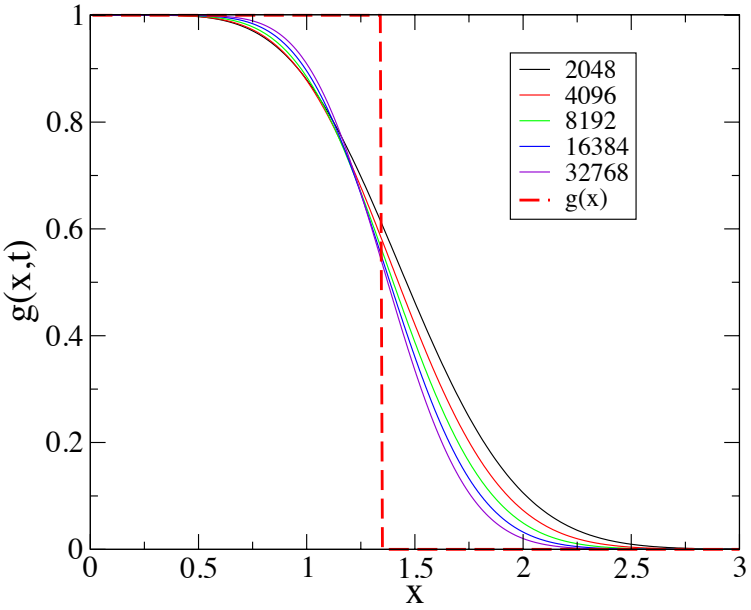

Figure 4. Function $g(x,t)$ against x for $t = 2048, 4096, \ldots, 32768$, obtained from the data of figure 2. The discontinuous curve is the limiting scaling function $g(x)$. The discontinuity is at $x_0 = (b(1+\sigma))^{1/(1+\sigma)}$, i.e., $x_0 = 1.341\ldots$ with $\sigma = 0.6$, $b = 1$.

4.3. Exact numerical results

We now compare the theoretical predictions above to the results of numerical integrations of the discrete master equation (3.1).

(i) Figure 2, already commented upon above, depicts $r_k(t)$ for the five different times $t = 2048$, 4096, 8192, 16384, 32768, for $\sigma = 0.6$, $b = 1$.

(ii) Figure 3 depicts the forward differences, $r_k(t) - r_{k+1}(t)$, of the previous data.

(iii) Figure 4 depicts the data of figure 2 plotted against x, i.e., $r_k(t) \approx g(x,t)$. The discontinuous curve is the limiting scaling function $g(x)$.

(iv) Figure 5 depicts the derivative $-g'(x,t)$ obtained by plotting the data of figure 3 against x. The location of the maximum is moving towards $x_0 = 1.341....$ The successive curves peak as $t^{a/2}$ towards the limiting function $\delta(x - x_0)$.

(v) Figure 6 gives a comparison between the theoretical prediction for $\varphi(x)$, obtained by a numerical integration of (4.23), with the results obtained from the data of

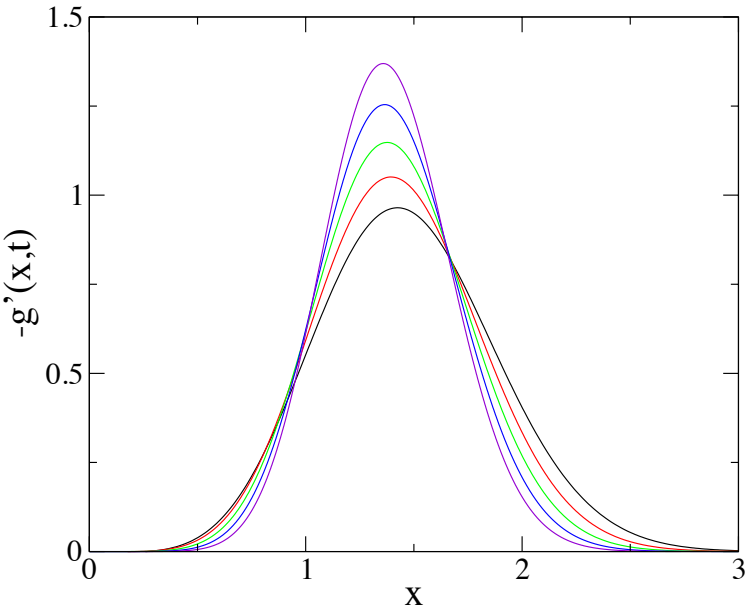

Figure 5. Function $-g'(x,t)$ for $t = 2048, 4096, \ldots, 32768$, obtained from the data of figure 4.

figure 4, using the definition (4.22). Note the perfect collapse of the latter onto a master curve, as well as their adequation with the former.

(vi) Figure 7 and 8 depict $g(x,t)$ and $-g'(x,t)$ against ξ, respectively, demonstrating the convergence of the data towards the theoretical prediction (4.29) and its derivative $\mathrm{e}^{-\xi^2}/\sqrt{\pi}$.

4.4. Using the sum rules

Taking into account the respective contributions of the two time-occupancy regimes (I) and (II), the sum rules (2.6) and (2.8) lead respectively to the following relationships,

$$0 = \sum_{k\geq 0}(f_k(t) - f_{k,\mathrm{eq}}) \approx \eta_t(v_0 + \rho_c) - I_0, \tag{4.33}$$

and

$$0 = \sum_{k\geq 1} k(f_k(t) - f_{k,\mathrm{eq}}) \approx \eta_t(v_0\rho_c + \mu_c) - I_1, \tag{4.34}$$

where $\mu_c = \langle N_1^2\rangle = \sum k^2 f_{k,\mathrm{eq}}$, and where the integrals I_0 and I_1 read

$$I_0 = \int_0^\infty \mathrm{d}k\, f_{k,\mathrm{eq}}(1 - g(k\varepsilon_t, t)), \tag{4.35}$$

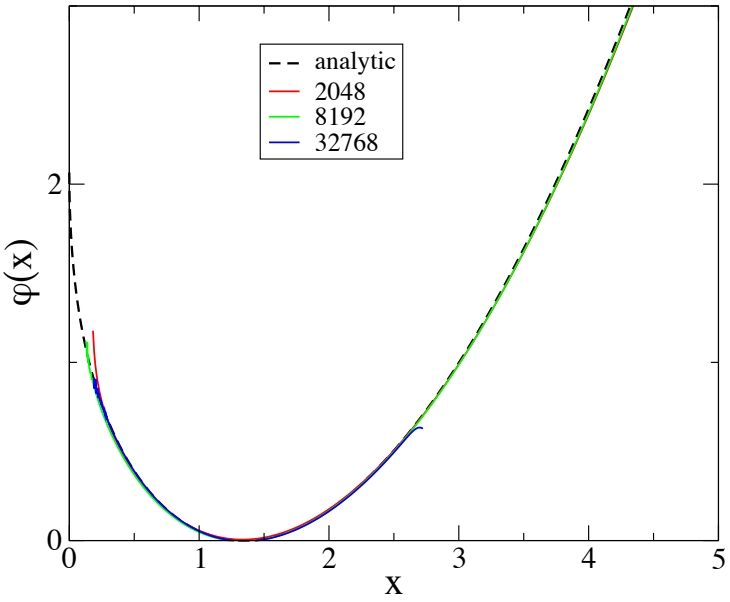

Figure 6. Comparison between the theoretical prediction for the large-deviation function $\varphi(x)$ given by (4.23) (dashed) with the results obtained from the data of figure 5, using the definition (4.22). These data have been shifted to x_0.

$$I_1 = \int_0^\infty \mathrm{d}k\, k\, f_{k,\mathrm{eq}}(1 - g(k\varepsilon_t, t)). \tag{4.36}$$

The integral I_0 is negligible compared to I_1 since the integrand of the latter bears an additional factor k, which is large. So, comparing (4.33) and (4.34), we conclude that

$$v_0 + \rho_c = 0. \tag{4.37}$$

So the proportionality constant between η_t and I_1 in (4.34) is the variance $\mu_c - \rho_c^2$.

We can now address the question of the time dependence of η_t. We have seen that in regime (I) (for k fixed, $t \to \infty$) $r_{k+1} - r_k \approx \eta_t$. On the other hand, in regime (II), for $x \to 0$, we have $r_{k+1} - r_k \sim g'(0,t)$. Since a matching mechanism between the two time-occupancy regimes (I) and (II) should take place, it is natural to suppose that

$$\eta_t \sim \mathrm{e}^{-t^a\, \varphi(0)}. \tag{4.38}$$

This result has been checked numerically. Looking at (4.34), we infer that

$$\eta_t \sim I_1 \sim \mathrm{e}^{-t^a\, \varphi(0)}. \tag{4.39}$$

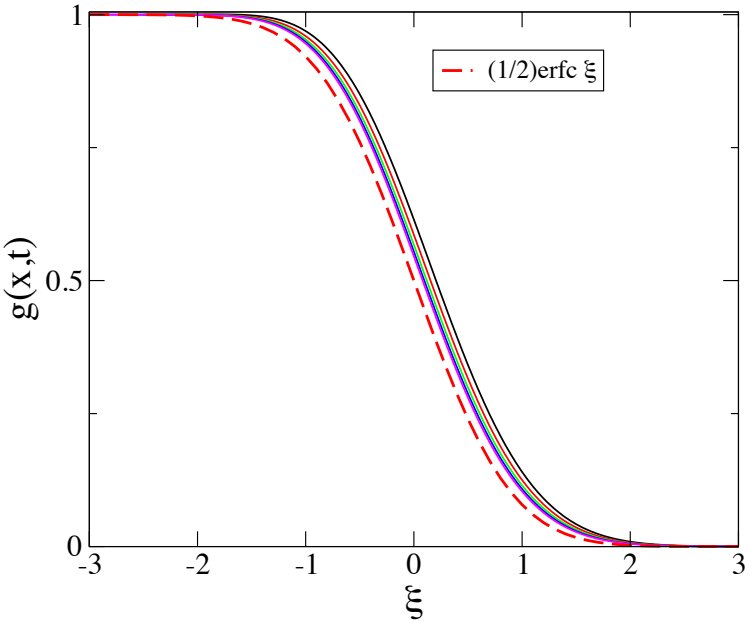

Figure 7. Same data as in figure 2, against scaling variable ξ defined in (4.30), compared to the bulk scaling function $(1/2)\,\mathrm{erfc}\,\xi$ (dashes).

5. Coarsening dynamics in the condensed phase

In this section we describe the dynamics of the ZRP in the condensed phase. As above, the system evolves from a homogeneous disordered initial condition, given e.g. by (4.1), now with an initial density $\rho > \rho_c$.

5.1. Time-occupancy regimes

Figure 9, obtained by numerical integration of the master equation (3.1), depicts $kf_k(t)$ against $\ln k$ for increasing times. These curves exhibit two well separated time-occupancy regimes: a first regime of convergence to equilibrium, before the dip, then a second regime corresponding to the bumps shifting progressively to the right. Rescaling k, as detailed below, we obtain figure 10 which indicates a slow convergence to a limiting curve (dashes).

These observations can be formalized as follows. We still set

$$\bar{u}_t = 1 + \eta_t, \tag{5.1}$$

where the small scale η_t will turn out to be different from its critical counterpart (4.2), and we investigate the dynamics according to two time-occupancy regimes, as for the critical case.

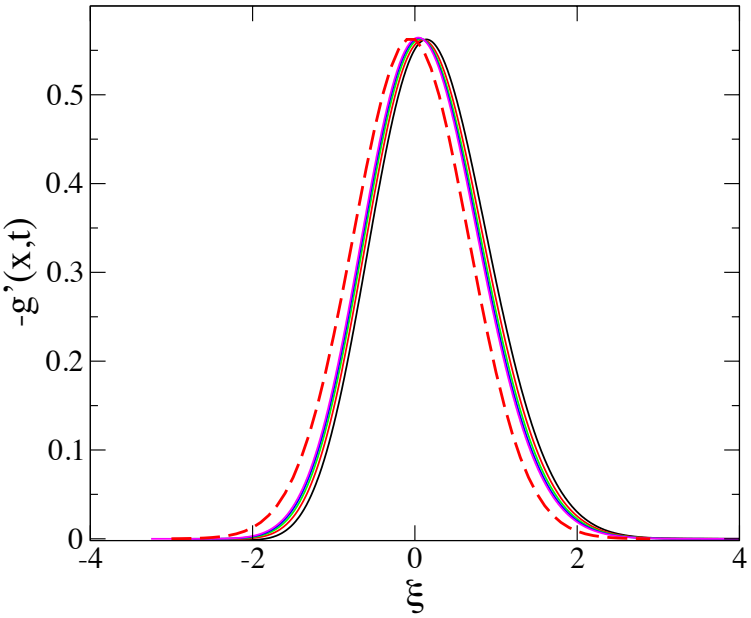

Figure 8. Same data as in figure 3 against ξ, compared to the Gaussian $\mathrm{e}^{-\xi^2}/\sqrt{\pi}$ (dashes). This function is normalised to unity with respect to ξ.

(I) *k fixed, t large* In this situation there is convergence to the equilibrium fluid phase and we still set

$$f_k(t) = f_{k,\mathrm{eq}}(1 + w_k(t)). \tag{5.2}$$

By the same reasoning as for the critical case we find, with $w_k = v_k \eta_t$, that

$$v_k = v_0 + k, \tag{5.3}$$

with v_0 given by (5.11), as demonstrated below.

(II) *k and t are simultaneously large* In the spirit of [6, 7] (see appendix), we look for a solution of (3.1) of the form

$$f_k(t) = \varepsilon_t^2 g(x,t), \quad x = k\varepsilon_t, \tag{5.4}$$

where x is the scaling variable and ε_t is a small scale which will turn out to be given again by (4.14). As in the critical case, $g(x,t)$ is expected to converge, in the limit of large times, to the scaling function $g(x)$, to be determined. In [6, 7] the explicit time dependence of $g(x,t)$ was not taken into account because the finite-time corrections were inessential.

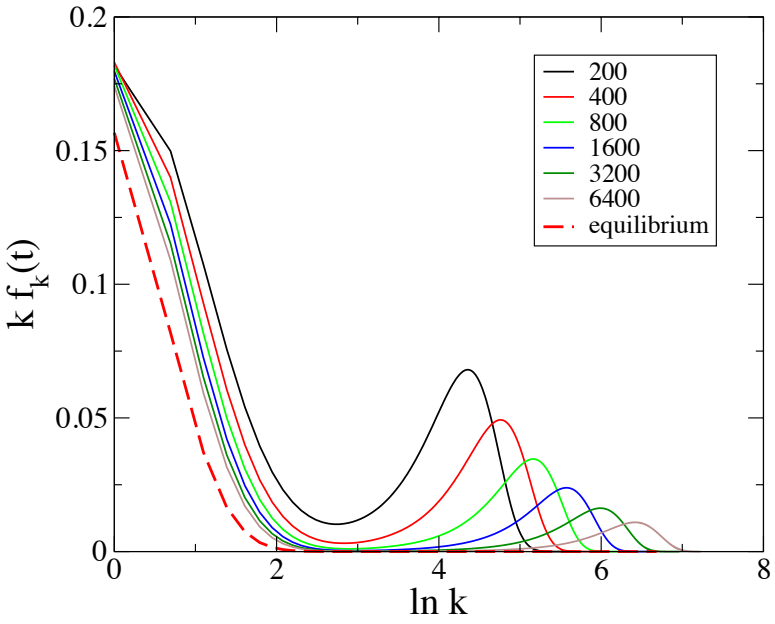

Figure 9. Product $kf_k(t)$ against $\ln k$ for $t = 200, 400, \ldots, 6400$. The dashed curve is the equilibrium distribution $f_{k,\mathrm{eq}}$. This figure substantiates the separation between the two time-occupancy regimes (I) and (II). Here $\sigma = 1/2, b = 4$, $\rho_c \approx 0.306$, $\rho = 20\rho_c$.

5.2. Using the sum rules

We start by using (5.2) and (5.4) as well as the sum rules (2.6) and (2.8) in order to derive (5.11) and (5.12). We proceed as follows. Let us mark the separation between the two time-occupancy domains by the position of the dip $k_\star$ clearly seen on figure 9. The first sum rule (2.6) leads to

$$1 = \sum_{k=0}^{k_\star} f_{k,\mathrm{eq}}\,(1 + \eta_t v_k) + \varepsilon_t^2 \sum_{k=k_\star}^{\infty} g(k\varepsilon_t, t), \tag{5.5}$$

hence

$$\eta_t \sum_{k=0}^{k_\star} f_{k,\mathrm{eq}}(v_0 + k) = -\varepsilon_t \int_{x_\star}^{\infty} \mathrm{d}x\, g(x,t) + \sum_{k=k_\star}^{\infty} f_{k,\mathrm{eq}}, \tag{5.6}$$

where $x_\star = k_\star \varepsilon_t^{-1}$. We then let $k_\star \to \infty$ and $x_\star \to 0$. This is justified by the fact that $k_\star$ increases much slower in time than ε_t^{-1}, as a simple argument shows (see the remark below). Thus

$$\eta_t(v_0 + \rho_c) = -\varepsilon_t \int_0^{\infty} \mathrm{d}x\, g(x,t). \tag{5.7}$$

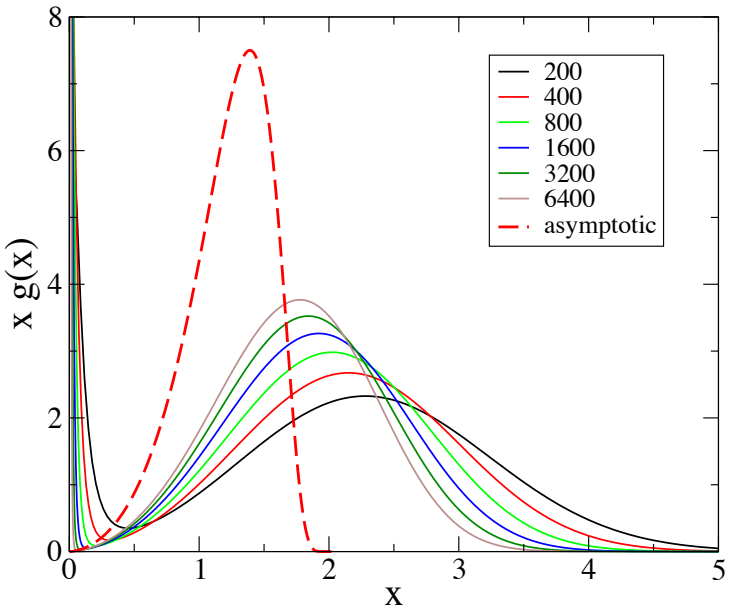

Figure 10. Same as figure 9 against the scaling variable x. The asymptotic dashed curve $xg(x)$ (6.4) is normalised according to (5.12).

The second sum rule (2.8) yields

$$\rho = \sum_{k=0}^{k_\star} k f_{k,\mathrm{eq}} \, (1 + \eta_t v_k) + \varepsilon_t^2 \sum_{k=k_\star}^{\infty} k g(k\varepsilon_t, t), \tag{5.8}$$

hence

$$\rho - \sum_{k=0}^{k_\star} k f_{k,\mathrm{eq}} = \eta_t \sum_{k=0}^{k_\star} k f_{k,\mathrm{eq}} (v_0 + k) + \int_{x_\star}^{\infty} \mathrm{d}x \, x g(x,t) \tag{5.9}$$

Thus

$$\rho - \rho_c = \eta_t (v_0 \rho_c + \mu_c) + \int_0^{\infty} \mathrm{d}x \, x g(x,t). \tag{5.10}$$

Taken together and assuming, as shown below, that $\eta_t \gg \varepsilon_t$, these equations impose the two constraints

$$v_0 + \rho_c = 0, \tag{5.11}$$

and

$$\rho - \rho_c = \int_0^{\infty} \mathrm{d}x \, x g(x,t). \tag{5.12}$$

Equation (5.11) determines v_0, while (5.12) gives the normalisation of the function $g(x,t)$ that we know investigate.

Remark In order to estimate the time dependence of $k_\star$ we impose the derivative of $f_k(t)$ with respect to k to vanish at this point. Using (2.12) and the fact that $g(x,t) \sim x^\sigma$ at large time (see section 6.1), we obtain

$$\mathrm{e}^{-b\,k_\star^{1-\sigma}/(1-\sigma)} \sim \varepsilon_t^{2+\sigma}, \tag{5.13}$$

hence

$$k_\star \sim (\ln t)^{1/(1-\sigma)}, \tag{5.14}$$

which is well verified numerically.

5.3. Equation satisfied by $g(x,t)$

Inserted into (3.1) the scaling form (5.4) yields a linear differential equation for $g(x,t)$. Indeed (3.1) can be rewritten as

$$\frac{\mathrm{d}f_k(t)}{\mathrm{d}t} = f_{k+1} + f_{k-1} - 2f_k + b\left(\frac{f_{k+1}}{(k+1)^\sigma} - \frac{f_k}{k^\sigma}\right) - \eta_t(f_k - f_{k-1}). \tag{5.15}$$

Replacing the discrete derivatives of f_k with respect to k by derivatives of $g(x,t)$ with respect to x, yields

$$\dot\varepsilon_t\varepsilon_t(2g + xg') + \varepsilon_t^2\dot g = \varepsilon_t^4 g'' + \varepsilon_t^{3+\sigma}\left(\frac{b}{x^\sigma} - \frac{\eta_t}{\varepsilon_t^\sigma}\right)g' - \varepsilon_t^{3+\sigma}\frac{\sigma b}{x^{1+\sigma}}g. \tag{5.16}$$

We divide both sides by $\varepsilon_t^{3+\sigma}$. Setting, as for the critical case,

$$\varepsilon_t = t^{-1/(1+\sigma)}, \tag{5.17}$$

implies $\dot\varepsilon_t/\varepsilon_t^{2+\sigma} = -1/(1+\sigma)$. Finally setting

$$\eta_t = A\,\varepsilon_t^\sigma, \tag{5.18}$$

where it is understood that A is a function of t, we obtain the continuum equation

$$t\dot g = t^{-a}g'' + \left(\frac{x}{1+\sigma} - A + \frac{b}{x^\sigma}\right)g' + \left(\frac{2}{1+\sigma} - \frac{\sigma b}{x^{1+\sigma}}\right)g, \tag{5.19}$$

with definition (4.16) for the exponent a. For $\sigma = 1$, omitting the left side of (5.19) we recover the equation corresponding to the ZRP with rate $u_k = 1 + b/k$, see (A.7). For this latter case, the term $t\dot g$ would give a finite-time correction to the scaling function $g(x)$. This was not considered in [5, 6, 7] because the convergence to $g(x)$ was very fast.

Remark A heuristic argument confirming the relationship (5.18) between η_t and ε_t is as follows. First, balancing $\bar u_t$ with u_k yields $k \sim \eta_t^{-1/\sigma}$. Then, noting that $k \sim \varepsilon_t^{-1}$ in the scaling region, (5.18) ensues.

6. Analysis of the continuum equation (5.19)

6.1. The scaling function

The stationary solution $g(x)$ of (5.19), obtained by letting $t \to \infty$, satisfies the equation

$$\left(\frac{x}{1+\sigma} - A + \frac{b}{x^\sigma}\right)g' + \left(\frac{2}{1+\sigma} - \frac{\sigma b}{x^{1+\sigma}}\right)g = 0, \tag{6.1}$$

which can be rewritten as

$$D(x)g' + \left(D'(x) + \frac{1}{1+\sigma}\right) g = 0, \tag{6.2}$$

where

$$D(x) = \frac{x}{1+\sigma} - A + \frac{b}{x^\sigma}. \tag{6.3}$$

The solution of this equation is

$$g(x) \propto \frac{1}{D(x)} \exp\left(-\frac{1}{1+\sigma}\int_0^x \mathrm{d}u \frac{1}{D(u)}\right). \tag{6.4}$$

If $x \to 0$ then $D(x) \sim x^{-\sigma}$, hence $g(x) \sim x^\sigma$. If $x \to \infty$ then $D(x) \sim x/(1+\sigma)$, thus

$$g(x) \sim \frac{1}{x} \mathrm{e}^{-\int^x \mathrm{d}u/u} \sim x^{-2}, \tag{6.5}$$

and therefore $\int \mathrm{d}x\, xg(x)$ diverges. This therefore rules out the possibility for $g(x)$ to have a support extending to infinity.

Let us more generally discuss which value of the amplitude A is selected. Denoting the value of x such that $D(x)$ is minimum by

$$x_0 = \left[b\,\sigma(1+\sigma)\right]^{\frac{1}{1+\sigma}}, \tag{6.6}$$

we have

$$D(x_0) = A_0 - A, \tag{6.7}$$

where

$$A_0 = \frac{x_0}{\sigma}. \tag{6.8}$$

Three cases are to be considered according to the sign of $D(x_0)$:

(i) $D(x_0) > 0$, or $A < A_0$,

(ii) $D(x_0) = 0$, or $A = A_0$,

(iii) $D(x_0) < 0$, or $A > A_0$.

Case (i) is necessarily ruled out since the support of $g(x)$ would extend to infinity. In case (iii) $g(x)$ would vanish at x_1, the first zero of $D(x)$. As will be demonstrated below, the selected solution is case (ii). For the latter, the asymptotic scaling function $g(x)$ has an essential singularity at x_0,

$$g(x) \sim \mathrm{e}^{-2x_0/((1+\sigma)(x_0-x))}, \tag{6.9}$$

and vanishes for $x > x_0$. The integral (6.4) is explicit when σ is rational. We plot $xg(x)$ for $\sigma = 1/2$ and $b = 4$ in figure 10, with the normalisation (5.12). Figure 10 also depicts $xg(x,t)$ for several values of time. One observes slow convergence to the asymptotic function $xg(x)$, that we now analyse.

6.2. A simplified form of (5.19)

Let us now analyse a simplified form of (5.19) where the left side, i.e., the $t\dot{g}$ term, is omitted. We rewrite the equation for convenience,

$$\gamma g'' + \left(\frac{x}{1+\sigma} - A + \frac{b}{x^\sigma}\right) g' + \left(\frac{2}{1+\sigma} - \frac{\sigma b}{x^{1+\sigma}}\right) g = 0, \tag{6.10}$$

where we have set $\gamma = t^{-a}$. Since the time dependence of $g(x,t)$ only enters through the small parameter γ, we denote the solution of (6.10) by $g(x,\gamma)$. The constraints on this function are that it should be positive and vanish at zero and infinity. This selects an amplitude A depending on γ, with limiting value A_0, when $\gamma \to 0$, as we now show.

We first cast (6.10) in normal form by setting $g(x,\gamma) = v(x)w(x)$, with $v(x)$ chosen in such a way that the resulting equation for w has no first derivative term. This gives

$$v(x) = \exp\left(-\frac{1}{2\gamma}\int_0^x \mathrm{d}u\, D(u)\right), \tag{6.11}$$

with

$$\int_0^x \mathrm{d}u\, D(u) = x\left(\frac{x}{2(1+\sigma)} - A + \frac{b}{(1-\sigma)x^\sigma}\right). \tag{6.12}$$

So

$$\begin{aligned} v(x) &\underset{x\to\infty}{\sim} \exp\left(-\frac{x^2}{4\gamma(1+\sigma)}\right), \\ v(x) &\underset{x\to 0}{\sim} \exp\left(-\frac{b\,x^{1-\sigma}}{2\gamma(1-\sigma)}\right). \end{aligned} \tag{6.13}$$

The equation for $w(x)$ reads

$$\gamma^2 w'' = \left(\frac{D(x)^2}{4} - \gamma\left(\frac{D'(x)}{2} + \frac{1}{1+\sigma}\right)\right) w, \tag{6.14}$$

which is a Schrödinger equation

$$\left(-\gamma^2 \frac{\mathrm{d}^2}{\mathrm{d}x^2} + V(x,A)\right) w = 0, \tag{6.15}$$

with potential

$$V(x,A) = \frac{1}{4}\left(\frac{x}{1+\sigma} - A + \frac{b}{x^\sigma}\right)^2 - \frac{\gamma}{2}\left(\frac{3}{1+\sigma} - \frac{\sigma b}{x^{1+\sigma}}\right). \tag{6.16}$$

We now analyse this equation in the semi-classical regime $\gamma \to 0$. In the ground state ($w(x)$ is positive), the particle sits at the minimum of the potential. Moreover, since this solution has zero energy, we have to express that this minimum vanishes, at leading order.

We expect this minimum to be located in the vicinity of x_0, with A close to A_0 because for $\gamma = 0$, $V(x,A)$ is minimum at x_0 (see (6.7)), and vanishes if $A = A_0$. We have

$$V(x_0,A) = \frac{(A-A_0)^2}{4} - \gamma\frac{1}{1+\sigma}. \tag{6.17}$$

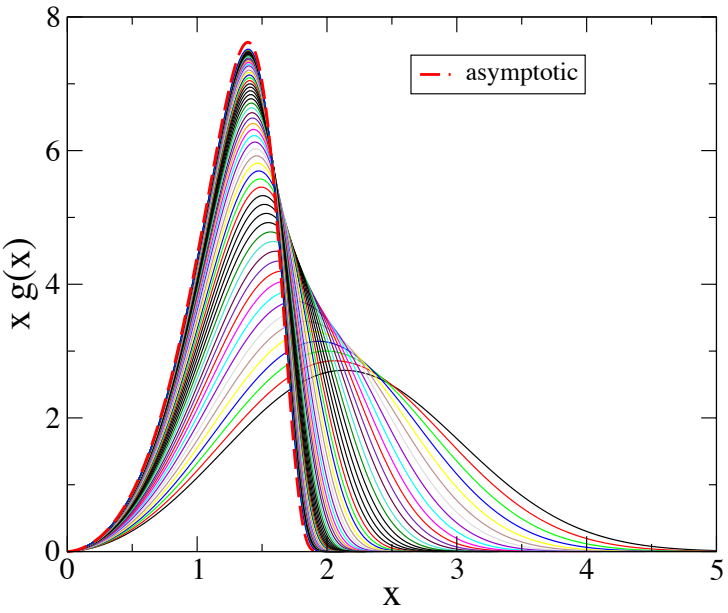

Figure 11. Solutions of the differential equation (6.10) obtained by numerical integration, for decreasing values of γ ($\sigma = 1/2, b = 4$), ranging from $\gamma = 0.4$ ($t \approx 15$) to $\gamma \approx 8.5\,10^{-6}$ ($t \approx 1.62\,10^{15}$).

Hence choosing $A = A_1 \equiv A_0 - 2\gamma^{1/2}/\sqrt{1+\sigma}$ yields $V(x_0, A_1) = 0$, and $V'(x_0, A_1) = -\gamma/(2x_0)$ (this last value is independent of A). We refine this analysis by expanding the potential around its minimum. We set

$$x = x_0 + \gamma^{3/8} z, \tag{6.18}$$

$$A = A_0 - \alpha\gamma^{1/2} + \beta\gamma^{3/4}, \tag{6.19}$$

where α and β will be determined. We obtain, for the potential, now a function of z,

$$\tilde{V}(z) = \frac{\gamma}{4}\left(\alpha^2 - \frac{4}{1+\sigma}\right) + \gamma^{5/4}\frac{\alpha}{4x_0}\left(z^2 - 2\beta x_0\right) + \cdots. \tag{6.20}$$

The leading order is suppressed by setting $\alpha = 2/\sqrt{1+\sigma}$, in agreement with the preliminary analysis made above. Finally (6.15) becomes the equation of a harmonic oscillator,

$$\left(-\frac{\mathrm{d}^2}{\mathrm{d}z^2} + \frac{\alpha}{4x_0}z^2\right)\tilde{w}(z) = \frac{\alpha\beta}{2}\tilde{w}(z), \tag{6.21}$$

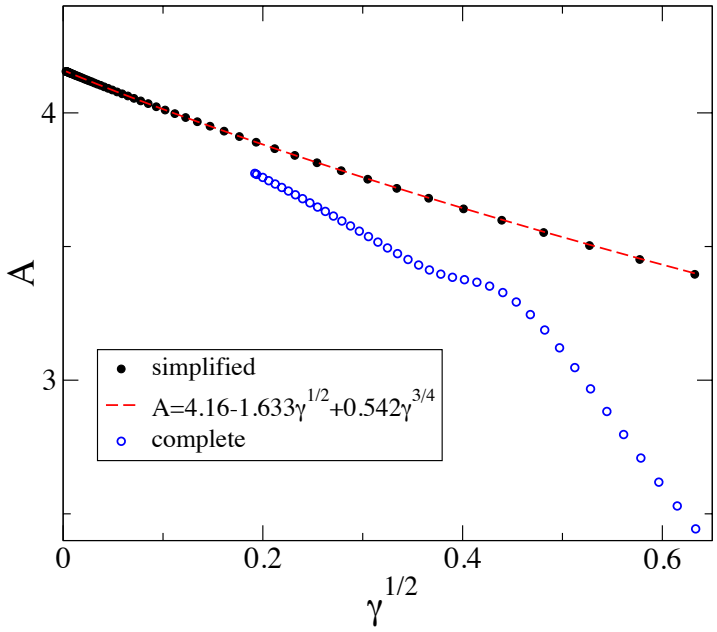

Figure 12. Upper curve: comparison between the amplitude A corresponding to the solutions, depicted in figure 11, of the simplified equation (6.10) (black dots) and the prediction (6.27) (red dashes). Lower curve: amplitude A obtained by numerical integration of the master equation (3.1) (the continuum limit of which is the complete equation (5.19)) (open blue dots).

with energy $\alpha\beta/2$. The ground-state solution is‡

$$\tilde{w}(z) \propto \exp\left(-\frac{cz^2}{2}\right), \tag{6.24}$$

that we cast in the equation above, in order to determine the constants c and β as,

$$c = \frac{1}{2}\sqrt{\frac{\alpha}{x_0}} = \frac{1}{\sqrt{2x_0}(1+\sigma)^{1/4}}, \quad \beta = \frac{2c}{\alpha}, \tag{6.25}$$

so (6.21) simplifies into

$$\left(-\frac{\mathrm{d}^2}{\mathrm{d}z^2} + c^2 z^2\right)\tilde{w}(z) = c\,\tilde{w}(z). \tag{6.26}$$

‡ Let us remind that the harmonic oscillator

$$-y'' + (x^2 - \lambda)y = 0, \tag{6.22}$$

with $y(\pm\infty) = 0$, has solutions in terms of Hermite polynomials, when $\lambda = 2n + 1$,

$$y_n(x) = \mathrm{e}^{-x^2/2} H_n(x). \tag{6.23}$$

Finally

$$A = A_0 - \frac{2}{\sqrt{1+\sigma}}\gamma^{1/2} + \frac{(1+\sigma)^{1/4}}{\sqrt{2x_0}}\gamma^{3/4} + \cdots . \tag{6.27}$$

Coming back to the original variable x, we have

$$w(x) \propto \exp\left(-\frac{c(x-x_0)^2}{2\gamma^{3/4}}\right). \tag{6.28}$$

The present analysis parallels that done for b large in the $\sigma = 1$ case, where the scaling function is found to have finite support with an essential singularity [6] (see the discussion below eq. (3.23) therein).

Let us compare these predictions to the results of a numerical integration of (6.10). Figure 11 depicts the solutions of this equation for various values of γ, ranging from $\gamma = 0.4$ ($t \approx 15$) to $\gamma \approx 8.5\,10^{-6}$ ($t \approx 1.62\,10^{15}$), with $\sigma = 1/2$ and $b = 4$. This figure demonstrates the very slow convergence of the finite-time solutions $g(x,t)$ to the stationary scaling function $g(x)$ given by (6.4) with $A = A_0$. The corresponding values of the amplitude A are depicted in figure 12 (black dots). These values are well predicted by (6.27) which yields $A \approx 4.160 - 1.633\gamma^{1/2} + 0.542\gamma^{3/4}$, with $\sigma = 1/2$ and $b = 4$ (red dashes).

6.3. Complete equation (5.19)

As can be seen in figure 12, the amplitude A obtained by numerical integration of the master equation (3.1) (yielding the complete equation (5.19) in the continuum limit) is different from the amplitude predicted for the simplified equation. This discrepancy is due to the finite-time corrections induced by the term $t\dot{g}$ in the left side of (5.19). The analysis of this situation is rather involved and is left for future work. As already mentioned earlier, for the $\sigma = 1$ case, finite-time corrections are also present. However these finite-time corrections are so small that there is no need to analyse their role.

7. Discussion

As mentioned in the introduction, the same condensing ZRP with rate (2.3) was recently investigated in [9], with focus on coarsening in the condensed phase. The scaling analysis of the single-site probability $f_k(t)$ given in this work turns out to be incorrect. In particular, the asymptotic scaling function $g(x)$ is not correctly predicted because A is not taken equal to A_0, as imposed by the selection mechanism described in section 6.1; for the analysis of the simplified equation (6.10) the time dependence of the amplitude A in (6.10) is overlooked (it is conjectured instead to be linear in b and depending on density, which does not hold); the complete equation (5.19) is not derived.

Acknowledgments

It is a pleasure to thank J M Luck for many enlightening discussions.

Appendix A. Summary of formula

We collect here some important formula for the ZRP under study, derived in the bulk of the paper, as well as the corresponding formula for the ZRP with rate $u_k = 1+b/k$, derived in [5, 6, 7], for comparison.

• *ZRP with rate* $u_k = 1 + b/k$

At criticality ($b > 3$)

$$\bar{u}_t = 1 + \eta_t, \quad \eta_t = A\varepsilon_t^{b-2}, \quad \varepsilon_t = t^{-1/2}. \tag{A.1}$$

$$f_k(t) = \begin{cases} f_{k,\mathrm{eq}}(1 + (v_0 + k)\eta_t) & : k \text{ fixed}, t \text{ large} \\ f_{k,\mathrm{eq}}\, g(k\varepsilon_t) & : k \text{ and } t \text{ large} \end{cases} \tag{A.2}$$

where $g(x)$ satisfies

$$g'' + \left(\frac{x}{2} - \frac{b}{x}\right) g' = 0, \tag{A.3}$$

and is explicitly given by [6]

$$g(x) = \frac{2^{-b}}{\Gamma(\frac{b+1}{2})} \int_x^\infty \mathrm{d}y\, y^b \mathrm{e}^{-y^2/4}. \tag{A.4}$$

The fall-off of $g(x)$ for $x \gg 1$ is very fast: $g(x) \sim \exp(-x^2/4)$, hence $f_k(t) \sim \exp(-k^2/4t)$. The amplitude A is a function of b alone and its explicit expression is known [6].

In the condensed phase

$$\bar{u}_t = 1 + \eta_t, \quad \eta_t = A\varepsilon_t, \quad \varepsilon_t = t^{-1/2}. \tag{A.5}$$

$$f_k(t) = \begin{cases} f_{k,\mathrm{eq}}(1 + (v_0 + k)\eta_t) & : k \text{ fixed}, t \text{ large} \\ \varepsilon_t^2 g(k\varepsilon_t) & : k \text{ and } t \text{ large} \end{cases} \tag{A.6}$$

where $g(x)$ is solution of the equation

$$g'' + \left(\frac{x}{2} - A + \frac{b}{x}\right) g' + \left(1 - \frac{b}{x^2}\right) g = 0. \tag{A.7}$$

The amplitude A is again a function of b alone. Its explicit expression is only known for large values of b [6].

• *ZRP with rate* $u_k = 1 + b/k^\sigma$

At criticality

$$\bar{u}_t = 1 + \eta_t, \quad \eta_t \sim \mathrm{e}^{-t^a \varphi(0)}, \quad \varepsilon_t = t^{-1/(1+\sigma)}. \tag{A.8}$$

$$f_k(t) = \begin{cases} f_{k,\mathrm{eq}}(1 + (v_0 + k)\eta_t) & : k \text{ fixed}, t \text{ large} \\ f_{k,\mathrm{eq}}\, g(k\varepsilon_t, t) & : k \text{ and } t \text{ large} \end{cases} \tag{A.9}$$

where $g(x,t)$ satisfies

$$t\dot{g} = t^{-a}\, g'' + \left(\frac{x}{1+\sigma} - \frac{b}{x^\sigma}\right) g', \tag{A.10}$$

with $a = (1-\sigma)/(1+\sigma)$.

In the condensed phase

$$\bar{u}_t = 1 + \eta_t, \quad \eta_t = A\varepsilon_t^\sigma, \quad \varepsilon_t = t^{-1/(1+\sigma)}. \tag{A.11}$$

$$f_k(t) = \begin{cases} f_{k,\mathrm{eq}}(1 + (v_0 + k)\eta_t) & : k \text{ fixed}, t \text{ large} \\ \varepsilon_t^2 g(k\varepsilon_t, t) & : k \text{ and } t \text{ large} \end{cases} \tag{A.12}$$

where $g(x,t)$ is solution of

$$t\dot{g} = t^{-a}\, g'' + \left(\frac{x}{1+\sigma} - A + \frac{b}{x^\sigma}\right) g' + \left(\frac{2}{1+\sigma} - \frac{\sigma b}{x^{1+\sigma}}\right) g. \tag{A.13}$$

References

[1] Spitzer F, 1970 Advances in Math. **5** 246
[2] Andjel E D, 1982 Ann. Prob. **10** 525
[3] Evans M R and Hanney T, 2005 J. Phys. A **38** R195
[4] Godrèche C, 2007 Lect. Notes Phys. **716** 261
[5] Drouffe J M, Godrèche C and Camia F, 1998 J. Phys. A **31** L19
[6] Godrèche C and Luck J M, 2001 Eur. Phys. J. B **23** 473
[7] Godrèche C, 2003 J. Phys. A **36** 6313
[8] Grosskinsky S, Schütz G M and Spohn H, 2003 J. Stat. Phys. **113** 389
[9] Jatuviriyapornchai W and Grosskinsky S, 2016 J. Phys. A **49** 185005
[10] Kafri Y, Levine E, Mukamel D, Schütz G M and Török J 2002 *Phys. Rev. Lett.* **89** 035702
[11] Godrèche C and Luck J M, 2005 J. Phys. A **38** 7215
[12] Evans M R, 2000 Braz. J. Phys. **30** 42
[13] Godrèche C and Luck J M, 2002 J. Phys.: Condens. Matter **14** 1601
[14] Bray A J, 1994 Adv. Phys. **43** 357
[15] Godrèche C and Luck J M, 2000 J. Phys. A **33** 9141
[16] Godrèche C and Luck J M, 2002 J. Phys. Cond. Matter **14** 1589
[17] Zwillinger D, 1997 *Handbook of differential equations* (Orlando, Florida: Academic press)